Sample Size Analysis of Energy Detection under Fading Channels

Miguel López-Benítez[†‡], Ogeen H. Toma[†], Dhaval K. Patel[*] and Kenta Umebayashi[§]
[†]Department of Electrical Engineering and Electronics, University of Liverpool, United Kingdom
[‡]ARIES Research Centre, Antonio de Nebrija University, Spain
[*]School of Engineering and Applied Science, Ahmedabad University, India
[§]Graduate School of Engineering, Tokyo University of Agriculture and Technology, Japan
Email: m.lopez-benitez@liverpool.ac.uk, ogeen.toma@liverpool.ac.uk, dhaval.patel@ahduni.edu.in, ume_k@cc.tuat.ac.jp

***Abstract*—The performance of energy detection under fading channels has been evaluated in terms of the average probability of detection as a function of the average Signal-to-Noise Ratio (SNR) and the channel fading parameters, assuming that the decision threshold is set to achieve a constant false alarm rate. However, the signal sample size, which is an important design parameter in the configuration of an energy detector and has a significant impact on its performance, has received no attention in the context of fading channels. The mathematical expressions available in the literature to calculate the sample size required to achieve desired target performance are valid for Additive White Gaussian Noise (AWGN) channels only, and the impact of fading on the required sample size remains unknown. In this context, this work fills the existing gap by providing analytical results that establish a direct relation between the channel fading parameters and the required sample size. The results are provided for a broad variety of fading models (Rayleigh, Nakagami-m, Nakagami-q/Hoyt, Nakagami-n/Rice, η–μ and κ–μ) in terms of elementary functions, which enables highly efficient numerical evaluations.**

***Index Terms*—Cognitive radio, dynamic spectrum access, spectrum sensing, energy detection, fading channels.**

I. Introduction

One of the most (if not the most) important requirements for Dynamic Spectrum Access / Cognitive Radio (DSA/CR) systems is to prevent harmful interference to licensed systems [1, 2]. To this end, DSA/CR systems are required to periodically monitor the idle/busy state of the licensed channel before attempting a transmission and vacate it as soon as the presence of a licensed signal is detected. A large variety of methods for signal detection, referred to as *spectrum sensing* in the context of DSA/CR, have been proposed in the literature [3–5]. While different sensing methods provide different trade-offs between detection performance and complexity, energy detection [6, 7] is typically preferred due to its low complexity and general applicability. Energy detection is the most popular sensing method in DSA/CR and is also employed in other systems where some form of signal detection is required [8].

Energy detection decides the presence or absence of a signal by comparing the energy of a finite set of signal samples to a predefined decision threshold. Thus, the decision threshold and the signal sample size are the two main design parameters that can be configured in an energy detector to achieve a desired target performance, which is typically expressed in terms of the probability of false alarm (probability to incorrectly declare an idle channel as busy) and the probability of detection (probability to correctly detect a busy channel as such). While the decision threshold can be set based on various criteria (e.g., see [9]), a common design criterion is to set the threshold so as to achieve a predefined probability of false alarm, which only requires the noise power to be known, and then set the sample size to guarantee a minimum probability of detection for a given minimum Signal-to-Noise Ratio (SNR).

While the design of the decision threshold has been extensively investigated (e.g., see [9]), the design of the sample size for the energy detector has not received sufficient attention. The sample size required by an energy detector to achieve a predefined target performance has been analysed under the Additive White Gaussian Noise (AWGN) channel model and closed-form expressions have been derived for such channel model. However, to the best of the authors' knowledge, no equivalent analytical results are available in the literature for fading channels. The analysis of energy detection under fading channels has focused on the evaluation of the average probability of detection as a function of the average SNR and the fading parameters, which has been extensively investigated for a wide variety of fading models and diversity reception techniques [10–15]. However, the sample size required by an energy detector to achieve a given target performance in the presence of fading does not appear to have been investigated to the date since the analytical results available in the literature are only valid for the AWGN channel model. Real-world wireless links are affected by fading and this has a significant impact on the performance of any wireless communication system, including DSA/CR systems and the signal detection (spectrum sensing) process itself. Taking into account that the sample size is an important design parameter in the configuration of an energy detector, the importance of having analytical results that can establish an explicit closed-form relation between the channel fading parameters and the required sample size becomes thus evident. This work fills the existing gap by providing such results for a broad variety of fading models, including Rayleigh, Nakagami-m, Nakagami-q (Hoyt), Nakagami-n (Rice), η–μ and κ–μ fading channels. Results are provided in terms of elementary functions, which allows for computationally efficient numerical evaluations.

The rest of this work is organised as follows. First, Section II presents the proposed evaluation approach, which relies on the derivation of expressions for the distribution of the sample

size, which are provided in Section III. Numerical results are provided in Section IV. Finally, Section V concludes this work.

II. Proposed Evaluation Approach

The sample size N required by an energy detector to achieve a probability of false alarm P_{fa} and a probability of detection P_d in an AWGN channel as a function of the instantaneous SNR per symbol γ is given by [16, eq. (9)]:

$$N = \left[\frac{\mathcal{Q}^{-1}(P_{fa}) - \mathcal{Q}^{-1}(P_d)(1+\gamma)}{\gamma}\right]^2 \tag{1}$$

where $\mathcal{Q}^{-1}(\cdot)$ denotes the inverse of the Gaussian Q-function $\mathcal{Q}(\cdot)$, defined in [17, eq. (26.2.3)].

One may attempt to evaluate the average sample size under fading by integrating (1) over the Probability Density Function (PDF) of the instantaneous SNR for the considered fading model, which is essentially the same approach commonly used in the literature to evaluate the average probability of detection under fading (e.g., see [10–15]). Unfortunately, this approach does not work in this case because the resulting integrals do not converge as a result of the infinite limit of (1) as $\gamma \to 0$.

This limitation is overcome in this work by means of a novel approach composed of two steps. The first step is to calculate the Cumulative Distribution Function (CDF) of the sample size, denoted as $F_N(N)$. Notice that in fading scenarios the instantaneous SNR γ will vary randomly according to a certain distribution given by the considered fading model. Thus, N in (1) can be seen as a function of the random variable γ and the definition of CDF can then be used to obtain $F_N(N)$ as:

$$\begin{aligned} F_N(N) &= P\left(\left[\frac{\mathcal{Q}^{-1}(P_{fa}) - \mathcal{Q}^{-1}(P_d)(1+\gamma)}{\gamma}\right]^2 \leq N\right) \\ &= P\Big(\gamma \geq \zeta(N)\Big) = \int_{\zeta(N)}^{\infty} f_\gamma(\gamma) d\gamma \end{aligned} \tag{2}$$

where $f_\gamma(\gamma)$ is the PDF of the instantaneous SNR per symbol for the considered channel fading model and $\zeta(N)$ is obtained after solving the inner inequality for γ, which yields:

$$\zeta(N) = \frac{\mathcal{Q}^{-1}(P_{fa}) - \mathcal{Q}^{-1}(P_d)}{\sqrt{N} + \mathcal{Q}^{-1}(P_d)} \tag{3}$$

It is worth mentioning that the lower integration limit of (2) implies $\zeta(N) \geq 0$, which is true given that the numerator and denominator of (3) are both positive. It can be shown that the probability of detection of an energy detector is lower bounded by its probability of false alarm (e.g., see [7, eq. (7)] and its limit as $\gamma \to 0$); hence $P_{fa} \leq P_d$ and the numerator of (3) is positive. The denominator will be positive if $N \geq [\mathcal{Q}^{-1}(P_d)]^2$, which is also true as it can be verified from (1):

$$N_{\min} = \min(N) = \lim_{\gamma \to \infty} N = [\mathcal{Q}^{-1}(P_d)]^2 \tag{4}$$

This is the lower bound of the domain over which $F_N(N)$ is defined. Thus, the expressions obtained from evaluating (2) are valid for $N \geq N_{\min}$, and $F_N(N) = 0$ for $N \leq N_{\min}$.

The second step of the proposed approach is to exploit the CDF obtained from (2) to evaluate the desired statistics. Since the CDF provides a complete characterisation of a random variable, it can be used to obtain a wide range of statistics. The moments can be obtained from the CDF as:

$$\mathbb{E}[N^k] = k \int_{N_{\min}}^{\infty} N^{k-1} \left[1 - F_N(N)\right] dN \tag{5}$$

a particular case of which is the mean sample size $\bar{N}$:

$$\bar{N} = \mathbb{E}[N] = \int_{N_{\min}}^{\infty} \left[1 - F_N(N)\right] dN \tag{6}$$

Moreover, it is straightforward to derive the maximum number of samples required for a given percentile $0 < \varepsilon < 1$ as:

$$N_{\max}^{(\varepsilon)} = F_N^{-1}(\varepsilon) \tag{7}$$

where $F_N^{-1}(\cdot)$ denotes the inverse of $F_N(\cdot)$. If $\varepsilon = 1/2$, then (7) provides the median sample size, $\tilde{N} = F_N^{-1}(1/2)$. The median is more robust to outliers than the mean (e.g., a few large values may significantly bias the mean of a set) and may therefore be better suited to characterise the central tendency of skewed distributions, which is the case of $F_N(N)$.

While the integral in (2) can be solved analytically for various fading models as it will be shown in Section III, the resulting expressions are in general too complex to enable an analytical evaluation of (5)–(7), except for some particular cases (e.g., Rayleigh and Nakagami-m). Therefore, in most cases (5)–(7) will have to be evaluated numerically based on the analytical result obtained from (2). A full numerical evaluation of the expressions involved in the two proposed steps would be possible as well, however this would have some notable disadvantages in terms of computational cost and required computation time. In particular, a numerical evaluation of (2) would in fact involve multiple numerical integrations, one for each value of N over which $F_N(N)$ needs to be evaluated (e.g., if the range of values of interest of N is represented by 10^3 points, then (2) would need to be evaluated 10^3 times). Therefore, the proposed approach based on the analytical resolution of (2) and the numerical evaluation of (5)–(7) can reduce dramatically the total computation time.

III. Distribution of the Sample Size under Fading

This section presents analytical results for (2) under various channel fading models. The analytical results are initially obtained in terms of mathematical functions that are defined as integrals and therefore require the use of numerical methods for their evaluation. To overcome this, alternative computationally efficient expressions in terms of elementary functions are provided as well. As discussed in Section II, the results presented in this section for $F_N(N)$ are valid for $N \geq N_{\min} = [\mathcal{Q}^{-1}(P_d)]^2$, while $F_N(N) = 0$ for $N \leq N_{\min}$.

A. Rayleigh Fading

Under Rayleigh fading, the instantaneous SNR per symbol is distributed according to [18, eq. (2.7)]:

$$f_\gamma(\gamma) = \frac{1}{\bar{\gamma}} \exp\left(-\frac{\gamma}{\bar{\gamma}}\right) \tag{8}$$

where $\bar{\gamma}$ is the average SNR. Introducing (8) in (2) yields the following expression for the distribution of the sample size:

$$F_N(N) = \exp\left(-\frac{1}{\bar{\gamma}}\zeta(N)\right) \tag{9}$$

Notice that the expression in (9) can be evaluated much more efficiently than the corresponding numerical integration of (2).

B. Nakagami-m Fading

Under Nakagami-m fading, the instantaneous SNR per symbol is distributed according to [18, eq. (2.21)]:

$$f_\gamma(\gamma) = \frac{m^m \gamma^{m-1}}{\bar{\gamma}^m \Gamma(m)} \exp\left(-\frac{m\gamma}{\bar{\gamma}}\right) \tag{10}$$

where $\bar{\gamma}$ is the average SNR, $m \geq 1/2$ is the Nakagami-m fading parameter and $\Gamma(\cdot)$ is the gamma function [17, eq (6.1.1)]. Introducing (10) in (2) leads to the following sample size distribution:

$$F_N(N) = 1 - P\left(m, \frac{m}{\bar{\gamma}}\zeta(N)\right) \tag{11}$$

where $P(\cdot,\cdot)$ represents the regularised lower incomplete gamma function [17, eq. (6.5.1)].

Notice that $P(\cdot,\cdot)$ is defined as a quotient of integrals and most commercial software packages evaluate this function by numerical methods. Some efficiency gains in computation time can be achieved by deriving an alternative closed-form expression in terms of elementary functions as follows. Introducing (10) into (2) leads to the following integral:

$$F_N(N) = \frac{m^m}{\bar{\gamma}^m \Gamma(m)} \int_{\zeta(N)}^{\infty} \gamma^{m-1} \exp\left(-\frac{m\gamma}{\bar{\gamma}}\right) d\gamma \tag{12}$$

The solution to the integral in (12) can be expressed in terms of the exponential integral function [17, eq. (5.1.4)], which is also defined as an integral and therefore would provide no advantage with respect to (11) in terms of computation efficiency. A computationally efficient expression can be obtained by solving the integral in (12) for integer values of m based on [17, eq (4.2.55)], which yields:

$$F_N(N) = \exp\left(-\frac{m}{\bar{\gamma}}\zeta(N)\right) \sum_{k=0}^{m-1} \frac{1}{k!} \left(\frac{m}{\bar{\gamma}}\zeta(N)\right)^k \tag{13}$$

The expression in (13) is based on elementary functions and can be evaluated efficiently, however it is valid only for integer values of m ($m \geq 1$). For non-integer values of m, (11) must be used at the expense of an increased computation time.

C. Nakagami-q (Hoyt) Fading

Under Nakagami-q (Hoyt) fading, the instantaneous SNR per symbol is distributed according to [18, eq. (2.11)]:

$$f_\gamma(\gamma) = \frac{1+q^2}{2q\bar{\gamma}} \exp\left(-\frac{(1+q^2)^2}{4q^2}\frac{\gamma}{\bar{\gamma}}\right) I_0\left(\frac{1-q^4}{4q^2}\frac{\gamma}{\bar{\gamma}}\right) \tag{14}$$

where $q \in [0,1]$ is the Nakagami-q fading parameter and $I_\nu(\cdot)$ is the νth-order modified Bessel function of the first kind [17, eq. (9.6.20)]. The associated CDF can be expressed as shown in [19, eq. (8)], which leads to the following result for (2):

$$F_N(N) = 1 - \mathcal{Q}\left(\alpha(q)\sqrt{\frac{\zeta(N)}{\bar{\gamma}}}, \beta(q)\sqrt{\frac{\zeta(N)}{\bar{\gamma}}}\right) + \mathcal{Q}\left(\beta(q)\sqrt{\frac{\zeta(N)}{\bar{\gamma}}}, \alpha(q)\sqrt{\frac{\zeta(N)}{\bar{\gamma}}}\right) \tag{15}$$

where $\mathcal{Q}(\cdot,\cdot)$ is the first-order Marcum Q-function [18, eq. (4.34)], and $\alpha(q)$ and $\beta(q)$ are given by[1]:

$$\alpha(q) = \frac{\sqrt{1-q^4}}{2q}\sqrt{\frac{1+q}{1-q}} \tag{16}$$

$$\beta(q) = \frac{\sqrt{1-q^4}}{2q}\sqrt{\frac{1-q}{1+q}} = \alpha(q)\frac{1-q}{1+q} \tag{17}$$

Since the Marcum Q-function is defined as an integral, the evaluation of the result in (15) can be inefficient when the number of points of N is large, which motivates the derivation of a more computationally efficient expression based on elementary functions as follows. Using [17, eq. (9.6.10)] and taking into account that $\Gamma(k+1) = k!$, the Bessel function $I_0(\cdot)$ can be written as:

$$I_0(x) = \sum_{k=0}^{\infty} \frac{\left(\frac{1}{2}x\right)^{2k}}{(k!)^2} \tag{18}$$

Introducing (18) in (14) and then in (2) leads to:

$$F_N(N) = \frac{1+q^2}{2q\bar{\gamma}} \sum_{k=0}^{\infty} \frac{1}{(k!)^2} \left(\frac{1-q^4}{8q^2\bar{\gamma}}\right)^{2k} \times \int_{\zeta(N)}^{\infty} \gamma^{2k} \exp\left(-\frac{(1+q^2)^2}{4q^2}\frac{\gamma}{\bar{\gamma}}\right) d\gamma \tag{19}$$

which can be solved using [17, eq (4.2.55)] to yield:

$$F_N(N) = \frac{2q}{1+q^2} \sum_{k=0}^{\infty} \left(\frac{1}{2}\frac{1-q^4}{(1+q^2)^2}\right)^{2k} \times e^{-\frac{(1+q^2)^2}{4q^2}\frac{\zeta(N)}{\bar{\gamma}}} \sum_{j=0}^{2k} \frac{(2k)!}{j!(k!)^2} \left(\frac{(1+q^2)^2}{4q^2}\frac{\zeta(N)}{\bar{\gamma}}\right)^j \tag{20}$$

Notice that the result in (20) is based on elementary functions. Moreover, it is valid for any value of the parameter q.

D. Nakagami-n (Rice) Fading

Under Nakagami-n (Rice) fading, the instantaneous SNR per symbol is distributed according to [18, eq. (2.16)]:

$$f_\gamma(\gamma) = \frac{(1+K)e^{-K}}{\bar{\gamma}} \exp\left(-(1+K)\frac{\gamma}{\bar{\gamma}}\right) \times I_0\left(2\sqrt{K(1+K)\frac{\gamma}{\bar{\gamma}}}\right) \tag{21}$$

where $K = n^2$ is the Rician K factor and $n \geq 0$ is the Nakagami-n fading parameter. The associated SNR CDF can

[1]The expressions provided in [19, eq. (8)] for $\alpha(q)$ and $\beta(q)$ are incorrect. The correct expressions are provided in the *erratum* published in [20].

be expressed in terms of the first-order Marcum Q-function [21, eq. (8)], which leads to the following result for (2):

$$F_N(N) = \mathcal{Q}\left(\sqrt{2K}, \sqrt{2(1+K)\frac{\zeta(N)}{\bar{\gamma}}}\right) \tag{22}$$

A more computationally efficient expression can be obtained by introducing (18) in (21) and then in (2), which leads to:

$$F_N(N) = e^{-K}\sum_{k=0}^{\infty}\frac{K^k}{(k!)^2}\left(\frac{1+K}{\bar{\gamma}}\right)^{k+1} \times \int_{\zeta(N)}^{\infty}\gamma^k \exp\left(-(1+K)\frac{\gamma}{\bar{\gamma}}\right)d\gamma \tag{23}$$

This integral can be solved using [17, eq (4.2.55)] to yield:

$$F_N(N) = e^{-K}\sum_{k=0}^{\infty}K^k \times e^{-(1+K)\frac{\zeta(N)}{\bar{\gamma}}}\sum_{j=0}^{k}\frac{1}{j!k!}\left((1+K)\frac{\zeta(N)}{\bar{\gamma}}\right)^j \tag{24}$$

Notice that the result in (24) is based on elementary functions. Moreover, it is valid for any value of the parameter $K = n^2$.

E. η-μ Fading

Under η-μ fading, the instantaneous SNR per symbol is distributed according to [22, eq. (26)]:

$$f_\gamma(\gamma) = \frac{2\sqrt{\pi}\mu^{\mu+\frac{1}{2}}h^\mu}{\Gamma(\mu)H^{\mu-\frac{1}{2}}}\frac{\gamma^{\mu-\frac{1}{2}}}{\bar{\gamma}^{\mu+\frac{1}{2}}}\exp\left(-2\mu h\frac{\gamma}{\bar{\gamma}}\right)I_{\mu-\frac{1}{2}}\left(2\mu H\frac{\gamma}{\bar{\gamma}}\right) \tag{25}$$

where η and μ are the fading parameters, and h and H are functions of η (see [22] for details). The CDF can be derived from [22, eq. (19)], which leads to the following result for (2):

$$F_N(N) = Y_\mu\left(\frac{H}{h}, \sqrt{2h\mu\frac{\zeta(N)}{\bar{\gamma}}}\right) \tag{26}$$

where $Y_v(\cdot,\cdot)$ is given by [22, eq. (20)]. The function $Y_v(\cdot,\cdot)$ is defined as an integral and its evaluation can be expected to be inefficient as a result. A computationally efficient expression can be obtained by introducing into (25) the following equality [17, eq. (9.6.10)]:

$$I_\nu(x) = \sum_{k=0}^{\infty}\frac{\left(\frac{1}{2}x\right)^{\nu+2k}}{k!\Gamma(\nu+k+1)} \tag{27}$$

and then the resulting expression into (2), which yields:

$$F_N(N) = 2\sqrt{\pi}\sum_{k=0}^{\infty}\frac{\mu^{2\mu+2k}h^\mu H^{2k}}{\Gamma(\mu)\Gamma(\mu+k+\frac{1}{2})\bar{\gamma}^{2\mu+2k}}\frac{1}{k!} \times \int_{\zeta(N)}^{\infty}\gamma^{2\mu+2k-1}\exp\left(-2\mu h\frac{\gamma}{\bar{\gamma}}\right)d\gamma \tag{28}$$

Since μ represents half the number of multipath clusters, 2μ takes integer values and so does $2\mu+2k-1$ ($\mu > 0$). Based on [17, eq (4.2.55)], the integral in (28) can be solved for integer values of $2\mu + 2k - 1$, which yields the following result:

$$F_N(N) = \sqrt{\pi}\sum_{k=0}^{\infty}\frac{H^{2k}}{\Gamma(\mu)\Gamma(\mu+k+\frac{1}{2})2^{2\mu+2k-1}h^{\mu+2k}} \times e^{-2\mu h\frac{\zeta(N)}{\bar{\gamma}}}\sum_{j=0}^{2\mu+2k-1}\frac{(2\mu+2k-1)!}{j!k!}\left(2\mu h\frac{\zeta(N)}{\bar{\gamma}}\right)^j \tag{29}$$

Notice that (29) is valid for integer values of 2μ. The μ fading parameter is intended to be the *real* extension of half the number of multipath clusters, which in theory should be an integer multiple of $1/2$ but in practice may not be for several reasons [22]. For non-integer values of 2μ, (26) must be used.

F. κ-μ Fading

Under κ-μ fading, the instantaneous SNR per symbol is distributed according to [22, eq. (10)]:

$$f_\gamma(\gamma) = \frac{\mu(1+\kappa)^{\frac{\mu+1}{2}}}{\kappa^{\frac{\mu-1}{2}}\exp(\mu\kappa)}\frac{\gamma^{\frac{\mu-1}{2}}}{\bar{\gamma}^{\frac{\mu+1}{2}}} \times \exp\left(-\mu(1+\kappa)\frac{\gamma}{\bar{\gamma}}\right)I_{\mu-1}\left(2\mu\sqrt{\kappa(1+\kappa)\frac{\gamma}{\bar{\gamma}}}\right) \tag{30}$$

where $\kappa, \mu > 0$ are fading parameters (see [22] for details). The corresponding CDF can be derived from [22, eq. (3)], which leads to the following result for (2):

$$F_N(N) = \mathcal{Q}_\mu\left(\sqrt{2\kappa\mu}, \sqrt{2(1+\kappa)\mu\frac{\zeta(N)}{\bar{\gamma}}}\right) \tag{31}$$

where $\mathcal{Q}_m(\cdot,\cdot)$ represents the generalised (mth-order) Marcum Q-function [18, eq. (4.60)]. A more computationally efficient expression can be obtained by introducing (27) in (30) and then in (2), which leads to the following integral:

$$F_N(N) = \sum_{k=0}^{\infty}\frac{\mu^{\mu+2k}\kappa^k(1+\kappa)^{\mu+k}}{\exp(\mu\kappa)\bar{\gamma}^{\mu+k}}\frac{1}{k!(\mu+k-1)!} \times \int_{\zeta(N)}^{\infty}\gamma^{\mu+k-1}\exp\left(-\mu(1+\kappa)\frac{\gamma}{\bar{\gamma}}\right)d\gamma \tag{32}$$

Since μ represents the number of multipath clusters, μ takes integer values and so does $\mu+k-1$ ($\mu > 0$). Based on [17, eq (4.2.55)], the integral in (32) can be solved for integer values of $\mu + k - 1$, which leads to the following result:

$$F_N(N) = \sum_{k=0}^{\infty}(\mu\kappa)^k e^{-\mu\kappa} \times e^{-\mu(1+\kappa)\frac{\zeta(N)}{\bar{\gamma}}}\sum_{j=0}^{\mu+k-1}\frac{1}{j!k!}\left(\mu(1+\kappa)\frac{\zeta(N)}{\bar{\gamma}}\right)^j \tag{33}$$

Notice that (33) is valid for integer values of μ. The μ fading parameter is intended to be the *real* extension of the number of multipath clusters, which in theory should be an integer number but in practice may be non-integer for various reasons [22]. For non-integer values of μ, (31) must be used.

IV. Numerical Results

This section follows the evaluation approach proposed in Section II along with the analytical results obtained in Section III to explore the impact of fading on the sample size that an energy detector requires to achieve a predefined target performance. The required sample size is here characterised by its median value. For random variables that take values within finite intervals, such as the probability of detection $P_d \in [0, 1]$, the mean may be a representative statistical average. However, for the sample size, which can take any value in the semi-infinite interval $[N_{\min}, \infty)$, the mean may be severely biased by very large (and unlikely) values. As discussed in Section II, the median is more robust to outliers than the mean and is thus better suited to describe the central tendency of skewed distributions, which is indeed the case for the sample size. For this reason, the median sample size is here considered.

Figs. 1 and 2 show the median sample size required by an energy detector to achieve $P_{fa} = 0.1$ and $P_d = 0.9$ under the considered fading models. As appreciated, the overall effect of fading is an increase in the required sample size with respect to the AWGN channel, which in some fading scenarios can be as large as ten times greater. This means that the well-known expression in (1) commonly considered in the literature would underestimate the required sample size and would thus lead to an under-performance of energy detection in real-world wireless communication channels. The results provided in this work can be used to estimate more accurately the actual sample size required in a broad range of fading channels.

The specific impact of fading for each channel fading model can be explained based on its parameters. In the Nakagami-m model, m quantifies the severity of fading. Fading is most severe for $m = 1/2$ (one-sided Gaussian model, i.e., the worst-case fading), equivalent to Rayleigh for $m = 1$, and converges to a non-fading AWGN channel as $m \to \infty$. This explains why the largest sample size under Nakagami-m fading is observed for $m = 1/2$ and decreases (converges to the AWGN curve) as m increases. The Nakagami-q (Hoyt) model spans the range from one-sided Gaussian fading ($q = 0$) to Rayleigh fading ($q = 1$), which explains the observed increase in the required sample size as q decreases. In the Nakagami-n (Rice) model, the parameter K (Rician factor) represents the ratio between the power in the direct Line-of-Sight (LoS) path and the power in the other (scattered) paths. $K = 0$ corresponds to a non-LoS scenario where all signal components are received through non-LoS scattered paths, which is indeed a Rayleigh fading scenario, equivalent to Nakagami-q (Hoyt) with $q = 1$. As the Rician factor increases ($K \to \infty$), the LoS component becomes predominant and converges to a constant-amplitude, non-fading AWGN scenario. This explains the reduction of the required sample size in Nakagami-n (Rice) fading as K increases. Fig. 2 shows that the η–μ (non-LoS) scenario in general requires a higher sample size than the κ–μ (LoS) counterpart, which can be explained by the fact that signal detection is more challenging under non-LoS conditions, thus requiring a larger sample size for the same detection performance. For the η–μ model, Format II is here considered, where η represents the correlation between the powers of the in-phase and quadrature scattered waves in each multipath cluster. Fig. 2 indicates that an increase in this correlation leads to an increase in the required sample size, which is compatible with the notion that for higher correlation among signal samples it is necessary to increase the sample size in order to have the same amount of uncorrelated observations of the fading process and achieve the same detection performance. In the κ–μ model, κ represents the ratio between the total power of the dominant components and the total power of the scattered waves. Similar to the case of Nakagami-n (Rice) fading, as the value of this ratio increases, the LoS components become predominant and the model converges to a constant-amplitude, non-fading AWGN scenario, where lower sample sizes are required. In both η–μ and κ–μ fading models, μ is related to the number of multipath clusters and an increase in its value implies a larger number of independent signal components at the receiver, which facilitates the detection of

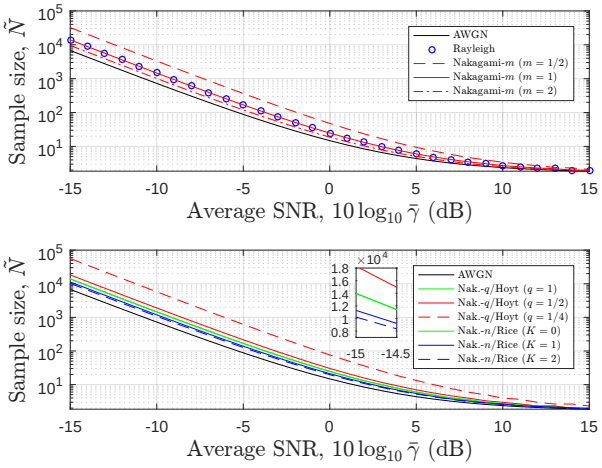

Fig. 1. Sample size required by an energy detector in Rayleigh, Nakagami-m, Nakagami-q (Hoyt) and Nakagami-n (Rice) fading.

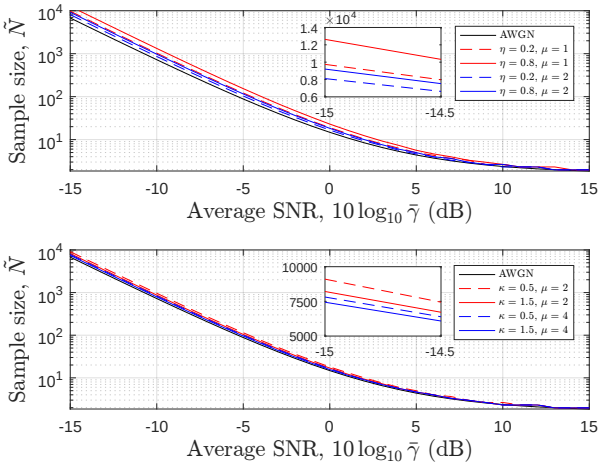

Fig. 2. Sample size required by an energy detector in η–μ and κ–μ fading.

TABLE I
COMPUTATION TIMES AVERAGED OVER 1000 ITERATIONS, WHEN N CONTAINS 1000 POINTS (AVERAGE SNR $10\log_{10}\bar{\gamma} = 0$ dB).

Fading model	Params.	Num. int. of (2)	Integral form	Series form
Nakagami-m	$m = 1$	4.56 s	(11) 0.21 ms	(13) 0.07 ms
Nakagami-q (Hoyt)	$q = 1/2$	38.00 s	(15) 15.29 ms	(20) 1.63 ms
Nakagami-n (Rice)	$K = 1$	48.51 s	(22) 8.01 ms	(24) 0.73 ms
η–μ	$\eta = 0.5$ $\mu = 1.5$	48.80 s	(26) 210.28 s	(29) 8.10 ms
κ–μ	$\kappa = 0.5$ $\mu = 3$	62.62 s	(31) 8.85 ms	(33) 3.98 ms

the received signal and reduces the required sample size. From the discussion above, it becomes apparent that the evaluation approach proposed in this work can be used to gain some insights on how the required sample size is affected by the fading process under different channel fading models.

Table I compares, for different fading models, the computation times required for the numerical integration of (2) and the evaluation of the analytical results obtained in this work, both in integral and series forms. For the series form, the minimum number of terms in the infinite sum that provides accurate results is considered (typically 5–10 terms). The results were obtained in Matlab with an Intel i7-2600 processor by averaging the computation times of 1000 repetitions when $F_N(N)$ is evaluated over 1000 values of N. As it can be appreciated, the numerical evaluation of (2) is highly inefficient since the integral needs to be solved numerically for every single value of N over which $F_N(N)$ is evaluated. The analytical results proposed in this work can reduce dramatically the required computation times, in particular the expressions in series form, which only involve elementary functions and are extremely efficient to evaluate. It is worth noting that the computation time for (26) is significantly higher than for the rest of counterparts in integral form. This is due to the need to implement $Y_v(\cdot,\cdot)$ [22, eq. (20)], while the rest of functions (Bessel, Marcum-Q and incomplete gamma functions) are built in Matlab and therefore evaluated much more efficiently. Thus, the analytical results obtained in this work not only allow the calculation of the sample size required by an energy detector under fading but do so in a highly efficient manner.

V. CONCLUSIONS

The sample size required by an energy detector in order to achieve a predefined target performance is a key parameter in the design and configuration of energy detection. The analytical results available in the literature to the date are only valid for the AWGN channel model and no results are known for fading scenarios. In this context, this work has investigated how the required sample size is affected by the presence of fading. The proposed evaluation approach and analytical results provided in this work can be used to estimate accurately and efficiently the required sample size for a broad range of channel fading models and therefore constitute a valuable tool in the design of the energy detector in real-world practical deployments. The impact of noise uncertainty has not been considered in this study but will be analysed in future work.

ACKNOWLEDGEMENTS

This work was supported by British Council under UKIERI DST Thematic Partnerships 2016-17 (ref. DST-198/2017).

REFERENCES

[1] Y.-C. Liang, K.-C. Chen, G. Y. Li, and P. Mähönen, "Cognitive radio networking and communications: An overview," *IEEE Trans. Vehic. Tech.*, vol. 60, no. 7, pp. 3386–3407, Sep. 2011.

[2] M. López-Benítez, "Cognitive radio," in *Heterogeneous cellular networks: Theory, simulation and deployment*. Cambridge University Press, 2013, ch. 13, pp. 383–425.

[3] T. Yücek and H. Arslan, "A survey of spectrum sensing algorithms for cognitive radio applications," *IEEE Commun. Surveys Tuts.*, vol. 11, no. 1, pp. 116–130, First Quarter 2009.

[4] E. Axell, G. Leus, E. G. Larsson, and H. V. Poor, "Spectrum sensing for cognitive radio: State-of-the-art and recent advances," *IEEE Signal Process. Mag.*, vol. 29, no. 3, pp. 101–116, May 2012.

[5] A. Ali and W. Hamouda, "Advances on spectrum sensing for cognitive radio networks: Theory and applications," *IEEE Commun. Surveys Tuts.*, vol. 19, no. 2, pp. 1277–1304, Second Quarter 2017.

[6] H. Urkowitz, "Energy detection of unknown deterministic signals," *Proc. IEEE*, vol. 55, no. 4, pp. 523–531, Apr. 1967.

[7] M. López-Benítez and F. Casadevall, "Improved energy detection spectrum sensing for cognitive radio," *IET Communications*, vol. 6, no. 8, pp. 785–796, May 2012.

[8] M. López-Benítez, "Overview of recent applications of cognitive radio in wireless communication systems," in *Handbook of Cognitive Radio*. Springer, 2018, pp. 1–32.

[9] M. López-Benítez and J. Lehtomäki, "Energy detection based estimation of primary channel occupancy rate in cognitive radio," in *Proc. IEEE Wireless Comms. and Networking Conf. (WCNC 2016), 2nd IEEE Int'l. Wksh. on Smart Spectrum (IWSS 2016)*, Apr. 2016, pp. 306–311.

[10] F. F. Digham, M.-S. Alouini, and M. K. Simon, "On the energy detection of unknown signals over fading channels," *IEEE Trans. Commun.*, vol. 55, no. 1, pp. 21–24, Jan. 2007.

[11] S. P. Herath, N. Rajatheva, and C. Tellambura, "Energy detection of unknown signals in fading and diversity reception," *IEEE Trans. Commun.*, vol. 59, no. 9, pp. 2443–2453, Sep. 2011.

[12] H. Sun, D. I. Laurenson, and C.-X. Wang, "Computationally tractable model of energy detection performance over slow fading channels," *IEEE Commun. Lett.*, vol. 14, no. 10, pp. 924–926, Oct. 2010.

[13] L. Gahane, P. K. Sharma, N. Varshney, T. A. Tsiftsis, and P. Kumar, "An improved energy detector for mobile cognitive users over generalized fading channels," *IEEE Trans. Commun.*, vol. 66, no. 2, pp. 534–545, Feb. 2018.

[14] A.-A. A. Boulogeorgos and G. K. Karagiannidis, "Energy detection in full-duplex systems with residual RF impairments over fading channels," *IEEE Wireless Commun. Lett.*, vol. 7, no. 2, pp. 246–249, Apr. 2018.

[15] M. Namdar and H. Ilhan, "Exact closed-form solution for detection probability in cognitive radio networks with switch-and-examine combining diversity," *IEEE Trans. Veh. Technol.*, vol. 67, no. 9, pp. 8215–8222, Sep. 2018.

[16] L. Rugini, P. Banelli, and G. Leus, "Small sample size performance of the energy detector," *IEEE Commun. Lett.*, vol. 17, no. 9, pp. 1814–1817, Sep. 2013.

[17] M. Abramowitz and I. A. Stegun, *Handbook of mathematical functions with formulas, graphs, and mathematical tables*, 10th ed. New York: Dover, 1972.

[18] M. K. Simon and M.-S. Alouini, *Digital communications over fading channels*, 2nd ed. Wiley-IEEE Pres, 2005.

[19] J. F. Paris, "Nakagami-q (Hoyt) distribution function with applications," *Electron. Lett.*, vol. 45, no. 4, pp. 210–211, Feb. 2009.

[20] ——, "Erratum," *Electron. Lett.*, vol. 45, no. 8, p. 432, Apr. 2009.

[21] M. Z. Bocus, C. P. Dettmann, and J. P. Coon, "An approximation of the first order Marcum Q-function with application to network connectivity analysis," *IEEE Commun. Lett.*, vol. 17, no. 3, pp. 499–502, Mar. 2013.

[22] M. D. Yacoub, "The κ-μ distribution and the η-μ distribution," *IEEE Antennas Propag. Mag.*, vol. 49, no. 1, pp. 68–81, Feb. 2007.